Int J Thermophys (2010) 31:2059–2077
DOI 10.1007/s10765-010-0889-3

Thermal Conductivity of Ionic Liquids: Measurement and Prediction

A. P. Fröba · M. H. Rausch · K. Krzeminski · D. Assenbaum · P. Wasserscheid · A. Leipertz

Received: 22 September 2010 / Accepted: 15 November 2010 / Published online: 1 December 2010

Abstract This study reports thermal-conductivity data for a series of [EMIM] (1-ethyl-3-methylimidazolium)-based ionic liquids (ILs) having the anions [NTf_2] (bis(trifluoromethylsulfonyl)imide), [OAc] (acetate), [$N(CN)_2$] (dicyanimide), [$C(CN)_3$] (tricyanomethide), [$MeOHPO_2$] (methylphosphonate), [$EtSO_4$] (ethylsulfate), or [$OcSO_4$] (octylsulfate), and in addition for ILs with the [NTf_2]-anion having the cations [HMIM] (1-hexyl-3-methylimidazolium), [OMA] (methyltrioctylammonium), or [BBIM] (1,3-dibutylimidazolium). Measurements were performed in the temperature range between (273.15 and 333.15) K by a stationary guarded parallel-plate instrument with a total measurement uncertainty of 3 % ($k = 2$). For all ILs, the temperature dependence of the thermal conductivity can well be represented by a linear equation. While for the [NTf_2]-based ILs, a slight increase of the thermal conductivity with increasing molar mass of the cation is found at a given temperature, the [EMIM]-based ILs show a pronounced, approximately linear decrease with increasing molar mass of the different probed anions. Based on the experimental data obtained in this

Electronic supplementary material The online version of this article (doi:10.1007/s10765-010-0889-3) contains supplementary material, which is available to authorized users.

A. P. Fröba (✉) · A. Leipertz
Erlangen Graduate School in Advanced Optical Technologies (SAOT),
University of Erlangen-Nuremberg, Paul-Gordan-Straße 6, 91052 Erlangen, Germany
e-mail: apf@aot.uni-erlangen.de

A. P. Fröba · M. H. Rausch · K. Krzeminski · A. Leipertz
Institute of Engineering Thermodynamics (LTT), University of Erlangen-Nuremberg,
Am Weichselgarten 8, 91058 Erlangen, Germany

D. Assenbaum · P. Wasserscheid
Institute of Chemical Reaction Engineering (CRT), University of Erlangen-Nuremberg,
Egerlandstraße 3, 91058 Erlangen, Germany

study, a simple relationship between the thermal conductivity, molar mass, and density is proposed for the prediction of the thermal-conductivity data of ILs. For this, also densities were measured for [EMIM][OAc], [EMIM][$C(CN)_3$], and [HMIM][NTf_2]. The mean absolute percentage deviation of all thermal-conductivity data for ILs found in the literature from the proposed prediction is about 7 %. This result represents a convenient simplification in the acquisition of thermal conductivity information for the enormous amount of structurally different IL cation/anion combinations available.

Keywords Density · Ionic liquids · Parallel-plate method · Prediction · Refractive index · Thermal conductivity

1 Introduction

The number of potential fields of application for ionic liquids (ILs) has strongly increased in recent years [1–6]. Beside their unique properties, this is mainly due to an almost unlimited number of possible IL cation/anion combinations which can be structurally tailored for a specific application. Current estimates of the number of possible ILs range between ten to the fourteenth to ten to the eighteenth [7]. To verify the applicability of a certain IL structure, e.g., as a solvent in catalytic reactions [8], entrainer in distillative separation [9], electrolyte in batteries [10], lubricant in difficult metal–metal wear contacts [11], or heat transfer fluid in energy technology [12], a detailed knowledge of its physical and chemical property profiles is required. The properties of every conceivable IL cannot be obtained by carrying out appropriate measurements, since this would represent a substantial investment in time and resources. Alternatively, an approach predicting the structure of an IL exhibiting the required set of properties would be very useful [13]. For this purpose, quantitative prediction methods with a reasonable uncertainty must be developed, see, e.g., [14–17]. Yet, all prediction methods can only be as accurate as the experimental data used for the evaluation of their performance. Although many physicochemical properties including equilibrium and transport properties of ILs have been studied extensively, a fundamental lack of reliable data still exists. In particular, only limited information on the thermal conductivity of ILs is available in the literature, although it is a key property in many engineering disciplines, e.g., in chemical process design [18]. At the present, a total amount of 242 experimental thermal-conductivity data points is available in the open literature for 28 pure ILs at atmospheric pressure [12,19–25].

The major aim of this study is to provide accurate and reliable data for the thermal conductivity of a set of pure ILs selected to cover a certain range of molecular weights from (170 to 650) $g \cdot mol^{-1}$. In detail, [EMIM] (1-ethyl-3-methylimidazolium)-based ILs carrying the anions [NTf_2] (bis(trifluoromethylsulfonyl)imide), [OAc] (acetate), [$N(CN)_2$] (dicyanimide), [$C(CN)_3$] (tricyanomethide), [$MeOHPO_2$] (methylphosphonate), [$EtSO_4$] (ethylsulfate), or [$OcSO_4$] (octylsulfate) were selected. Moreover, a series of ILs with the [NTf_2]-anion combined with the cations [HMIM] (1-hexyl-3-methylimidazolium), [OMA] (methyltrioctylammonium), or [BBIM] (1,3-dibutylimidazolium) was investigated. With the obtained experimental data, a simple prediction method for the thermal conductivity of ILs is developed and compared with the thermal-conductivity data of other ILs available from the literature.

2 Experimental

2.1 Materials and Sample Preparation

[EMIM][$N(CN)_2$], [EMIM][$MeOHPO_2$], and [EMIM][NTf_2] were purchased from Solvent Innovation GmbH, Cologne, Germany. [EMIM][OAc] and [EMIM][$C(CN)_3$] were purchased from BASF AG, Germany, and Lonza Cologne AG, Germany. [EMIM][$EtSO_4$] was obtained by the synthesis procedure described by Maier et al. [26]. [EMIM][$OcSO_4$] was synthesized by reacting [EMIM][$EtSO_4$] with *n*-octanol with the procedure described by Himmler et al. [27]. For the synthesis of [BBIM][NTf_2], the procedure described in our former work [28] was used. [HMIM][NTf_2] was obtained by applying the same method using the reactants [HMIM][Cl] (1-hexyl-3-methylimidazolium chloride) and [Li][NTf_2] (lithium bis(trifluoromethylsulfonyl)imide). [HMIM][Cl] was previously synthesized by reaction of methylimidazole with 1-chlorohexane as described by Davis et al. [29]. [OMA][NTf_2] was obtained by a two-step synthesis. First, methyltrioctylammonium methylsulfate was produced by reacting trioctylamine with dimethylsulfate at equimolar conditions. This procedure has to be carried out very carefully with cooling due to the strongly exothermic character of the reaction. The second step is an ion exchange in distilled water with lithium bis(trifluoromethylsulfonyl)imide. The resulting denser phase is the formed product [OMA][NTf_2], and the upper phase consists of the exchanged ions and water. To improve purity, the product was washed with distilled water several times and dried under vacuum at 60 °C.

The purities of the synthesized ILs were proven by ^{1}H NMR analysis (JEOL, ECX +400 spectrometer) with dimethylsulfoxide-d_6 (DMSO-d_6) as a solvent. The total peak integral in the ^{1}H NMR spectrum was used to determine the nominal purities of the ILs on a molar basis. Prior to use, all ILs were dried at about 333.15 K for a time period of at least 4 h on a vacuum line (0.5 mbar) with an oil-sealed vacuum pump and a liquid nitrogen trap. For the dried ILs, the water mass fraction was determined by Karl Fischer coulometric titration (Metrohm, 756 KF Coulometer) directly before filling the sample cell of the parallel-plate instrument. The expanded relative uncertainty ($k = 2$) of the water content determinations performed within this work depends on the water mass fraction and is estimated to be between ±20 % and ±5 %, corresponding to water mass fractions ranging from 4.0×10^{-4} to 5.0×10^{-2}. For lower mass fractions, the relative uncertainty was about ±20 %. The molecular weights, nominal purities, and water mass fractions of the studied ILs are summarized in Table 1. All parts of the measuring devices which were in contact with the sample as well as all glassware used for sample handling were cleaned, rinsed with double-distilled water, and oven-dried.

2.2 Parallel-Plate Instrument for Measuring the Thermal Conductivity

For measuring the thermal conductivity λ_c of the ILs, a parallel-plate instrument applicable to fluids as well as thin solid bodies and bulk solids was used, see Fig. 1. It is designed to fulfill the ideal one-dimensional form of the Fourier law of heat conduction for a planar sample,

Table 1 Molecular weight M, nominal purity on a molar basis, and water mass fraction w of the ILs studied in this work

IL	M (g · mol^{-1})	Purity (mol%)	w
[EMIM][OAc]	170.21	>98	9.36×10^{-3}
[EMIM][N(CN)$_2$]	177.20	>98	1.03×10^{-3}
[EMIM][C(CN)$_3$]	201.24	>98	5.55×10^{-4}
[EMIM][MeOHPO$_2$]	206.18	>98	2.32×10^{-4}
[EMIM][EtSO$_4$]	236.30	>99	2.18×10^{-3}
[EMIM][OcSO$_4$]	320.45	>99	1.32×10^{-3}
[EMIM][NTf$_2$]	391.30	>99	3.33×10^{-4}
[HMIM][NTf$_2$]	447.42	>98	8.60×10^{-5}
[BBIM][NTf$_2$]	461.44	>99	1.19×10^{-4}
[OMA][NTf$_2$]	648.90	>98	7.81×10^{-4}

$$\dot{Q} = A\frac{\lambda_c}{s}\Delta T, \tag{1}$$

as close as possible. In Eq. 1, $\dot{Q}$ is the heat flowing through a sample with heat transfer area A and thickness s when the temperature difference ΔT is applied between the two outer surfaces of the sample. In this study, an IL layer located in a narrow gap between two horizontal plates is subjected to a stationary temperature gradient. The temperature gradient is adjusted by controlling the temperatures of the upper (diameter 86 mm) and lower (diameter 146 mm) plate. The upper plate is kept at the higher temperature to keep free convection in the fluid layer to a minimum. For this, also any deviation from a horizontal arrangement has to be avoided by carefully adjusting the plates. Furthermore, the smaller diameter of the balanced heating plate minimizes effects of convective flows occurring at the boundary of the fluid volume on the heat flow through the sample. Convective heat transfer increases with increasing values of the dimensionless Rayleigh number;

$$Ra = \frac{g\alpha_p \Delta T s^3 c_p \rho^2}{\lambda_c \eta}, \tag{2}$$

where g is the gravitational constant, and α_p, c_p, ρ, and η are the thermal expansion coefficient, the specific heat at constant pressure, the density, and the dynamic viscosity of the fluid, respectively. Naziev et al. [30] stated that for vertical coaxial cylinders, convective heat transfer can be neglected for $Ra < 1000$. For the horizontal parallel-plate arrangement used here, however, the critical Rayleigh number must be distinctly larger. The Rayleigh number of the ILs studied in this work could be estimated to be in the range between 0.01 and 100. Consequently, convective heat transfer between the heating and the cooling plate can be neglected for the present measurements.

For ensuring that the heating power provided in the upper plate only results in a heat flow through the fluid layer to the lower plate, the upper plate is surrounded by a guard system. This system consists of a guard ring in which the balanced heating plate

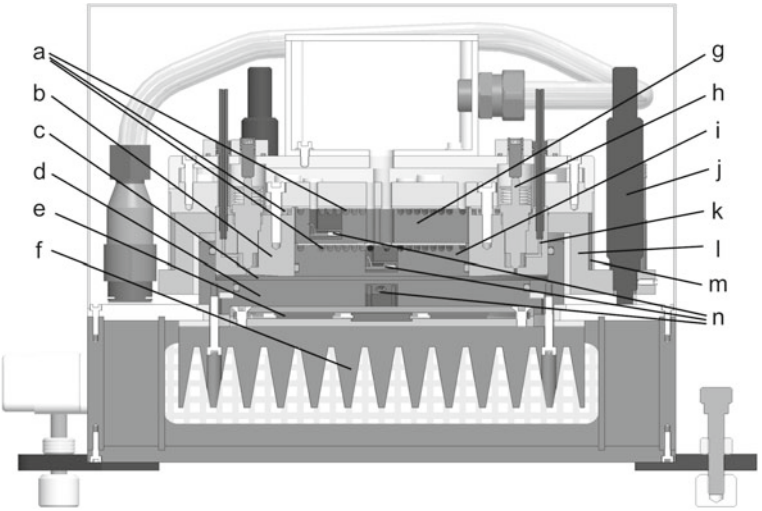

Fig. 1 Guarded parallel-plate instrument for the measurement of thermal conductivity: (*a*) heating wires; (*b*) guard ring; (*c*) liquid sample layer; (*d*) cooling plate; (*e*) Peltier elements; (*f*) fins cooled by fans; (*g*) upper guard plate; (*h*) valves; (*i*) heating plate; (*j*) micrometer screws; (*k*) filling lines; (*l*) outer guard ring; (*m*) heating foil; (*n*) Pt 100 Ω resistance probes

is immersed and a guard plate located above the heating plate. Another guard ring surrounding the complete upper part of the instrument minimizes effects of the ambient conditions on the temperature control system. All parts of the guard system are kept to the same temperature as the upper plate. While the temperature control for the guard rings and guard plate as well as for the balanced upper plate is realized by resistance heating, the lower plate of the apparatus can be heated or cooled by Peltier elements. For measurements below room temperature, the complete parallel-plate instrument is surrounded by an insulating housing which can be cooled by a lab thermostat to about 10 K below the desired temperature inside the liquid layer.

The heat flow $\dot{Q}$ provided by the upper plate and conducted through the sample is determined by measuring the electric power dissipated in the corresponding resistance heating. This heating is realized by a resistance wire connected to a DC power supply (Agilent E3645A) using a four-wire system. The power supply provides voltage and electric current data with relative uncertainties ($k = 2$) of ± 0.05 % and ± 0.15 %, allowing the calculation of the electric power dissipated in the heating plate with an estimated relative uncertainty smaller than 0.2 %. For evaluation of the thermal conductivity according to Eq. 1—beside the effective area A of the heating plate—the thickness of the fluid layer s and the surface temperatures of the plates are required. The layer thickness can be adjusted by three micrometer screws with an estimated uncertainty of ± 0.01 mm. The surface temperatures of the plates contacting the sample are extrapolated from the absolute temperatures and axial temperature gradients inside the plates. These are measured with pairs of temperature probes inserted into high precision bores which are located along the plate axis. Platinum resistance probes of 100 Ω were used for all temperature measurements in the instrument. Before use,

the resistance probes including the whole cabling of the four-wire system were calibrated, resulting in an absolute uncertainty of ±0.01 K. The relative uncertainty of the resistance probes among each other was smaller than ±0.005 K.

The parallel plates and the bodies of the guard system are made of copper. The copper surfaces which are in contact with the sample fluid were polished and covered with a thin chrome layer. Thus, the radiative contribution to the total heat flow is small when compared to that caused by heat conduction. Nevertheless, radiation corrections are necessary for obtaining precise thermal-conductivity data for weakly absorbing fluids such as ILs. For these fluids, the effective thermal conductivity λ_{eff} measured in a parallel-plate instrument consists of contributions of conductive (λ_{c}) and radiative (λ_{r}) heat transfer,

$$\lambda_{\mathrm{eff}} = \lambda_{\mathrm{c}} + \lambda_{\mathrm{r}}. \tag{3}$$

For the determination of λ_{r}, an approximate calculation method proposed by Braun et al. [31] can be used. It is based on a mathematical model for small temperature differences developed by Kohler [32] and Poltz [33] and implies some simplifications. The latter include a linear temperature distribution in the sample and a constant emission coefficient of $\varepsilon = 0.04$ for the polished and chromed plate walls which are in contact with the fluid. With the transmissions $D(\nu)$ for the wave numbers, ν, λ_{r} can be determined,

$$\lambda_{\mathrm{r}} = \frac{4}{3} c_1 c_2 n^2 \int_{\nu=\infty}^{0} s_0 \frac{Y(\tau,\varepsilon)}{\ln D(\nu)} \frac{\nu^4 \exp\left(\frac{\nu c_2}{\bar{T}}\right)}{\bar{T}^2\left[\exp\left(\frac{\nu c_2}{\bar{T}}\right)-1\right]^2} \,\mathrm{d}\nu. \tag{4}$$

$c_1 (= 3.741771 \times 10^{-16}\ \mathrm{W \cdot m^2})$ and $c_2 (= 1.43877 \times 10^{-2}\ \mathrm{m \cdot K})$ are the constants in Planck's spectral energy distribution, and $\bar{T}$ denotes the mean temperature of the fluid. As infrared refractive-index data n for the ILs used here are not available in the literature and cannot be easily measured, the values at the sodium vapor line for the mean temperature of all thermal-conductivity measurements of 313.15 K provided in our former studies [28,34] were used. As [EMIM][OAc], [EMIM][C(CN)$_3$] and [HMIM][NTf$_2$] were not part of these studies, their refractive indices n_{D} for the sodium vapor line ($\lambda_{\mathrm{D}} = 589.3$ nm) and refractive index differences $n_{\mathrm{F}} - n_{\mathrm{C}}$ for the Fraunhofer lines F ($\lambda_{\mathrm{F}} = 486.1$ nm) and C ($\lambda_{\mathrm{C}} = 656.3$ nm) were determined and correlated with the same method. The results obtained for n_{D} and $n_{\mathrm{F}} - n_{\mathrm{C}}$ at atmospheric pressure in the temperature range from (283.15 to 313.15) K with an Abbé refractometer (Leo Kuebler, R 6000 G) with expanded uncertainties ($k = 2$) of less than ±0.0005 and ±0.001 are listed in Table 2. The refractive index n_{calc} can be calculated by the linear equation;

$$n_{\mathrm{calc}} = n_0 + n_1 T + \frac{n_{\mathrm{F}} - n_{\mathrm{C}}}{\lambda_{\mathrm{F}} - \lambda_{\mathrm{C}}} (\lambda - \lambda_{\mathrm{D}}), \tag{5}$$

where T represents the temperature in K and λ is the wavelength for which the refractive index is calculated in m. The fit parameters n_0 and n_1 as well as the mean dispersion

Table 2 Refractive index n_D and refractive-index difference $n_F - n_C$ of [EMIM][OAc], [EMIM][C(CN)$_3$], and [HMIM][NTf$_2$] at temperature T and atmospheric pressure

T (K)	[EMIM][OAc]		[EMIM][C(CN)$_3$]		[HMIM][NTf$_2$]	
	n_D	$n_F - n_C$	n_D	$n_F - n_C$	n_D	$n_F - n_C$
283.15	1.5030	0.0124	1.5154	0.0143	1.4355	0.0096
293.15	1.5002	0.0121	1.5139	0.0140	1.4324	0.0098
303.15	1.4981	0.0118	1.5110	0.0142	1.4298	0.0080
313.15	1.4950	0.0116	1.5084	0.0143	1.4271	0.0080

Table 3 Coefficients of Eq. 5 for the refractive index n_{calc} of [EMIM][OAc], [EMIM][C(CN)$_3$], and [HMIM][NTf$_2$]

	n_0	n_1 (K^{-1})	$(\Delta n/\Delta\lambda)$ (m^{-1})	rms[a]
[EMIM][OAc]	1.57689	−0.000261	−70347	0.014
[EMIM][C(CN)$_3$]	1.58343	−0.000239	−83320	0.022
[HMIM][NTf$_2$]	1.51409	−0.000278	−51988	0.008

[a] Standard percentage deviation of n_D to the fit

$(n_F - n_C)/(\lambda_F - \lambda_C)$ are given in Table 3. The mean dispersion corresponds to the average value of the refractive index differences $n_F - n_C$ and is assumed to be independent of the temperature. For all ILs, the deviations of the experimental refractive-index data n_D from the correlation according to Eq. 5 are clearly within the measurement uncertainty.

In Eq. 4, the reflectance of the fluid Y is a function of the emission coefficient ε and the optical thickness τ and has been calculated and tabulated by Poltz [33]. τ can be determined with the layer thickness s_0 used for the measurement of the transmission spectra,

$$\tau = -\frac{s}{s_0} \ln D. \tag{6}$$

The transmission spectra of the ILs studied in this work were measured with a Fourier transform infrared spectrometer (JASCO FT/IR4100) for wave numbers ν ranging from (700 to 4000) cm^{-1} and a layer thickness of $s_0 = 1$ μm at a temperature of 293.15 K. The spectra are presented in Fig. 2. The corresponding data are available as electronic supplemental material. It should be noted that for wave numbers between (2300 and 2390) cm^{-1}, the transmission was set to unity. In this range of ν, the spectrometer hardly allows any transmission, resulting in artifacts with apparent transmissions significantly larger than unity for the fluids. Only for [EMIM][MeOHPO$_2$], small absorption rates were found for the corresponding wave numbers. Evaluation of the spectrum with and without the described correction, however, did not affect the result for λ_r significantly. For all ILs studied within this work, the radiative heat transfer represented by λ_r makes up (0.20 to 1.28) % of the effective thermal conductivity measured.

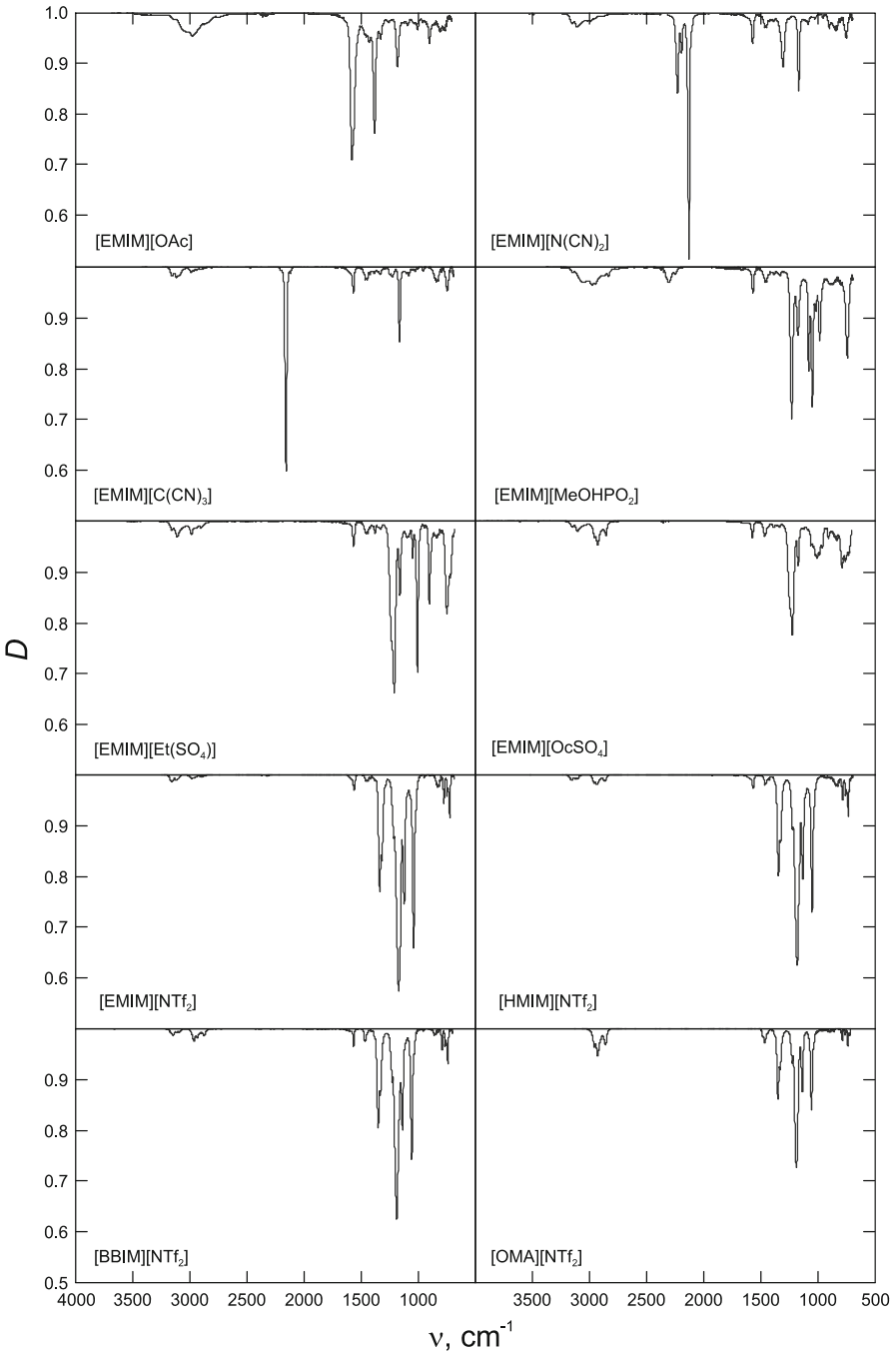

Fig. 2 Transmission spectra of the studied ILs obtained for a layer thickness of 1 μm at a temperature of 293.15 K and atmospheric pressure

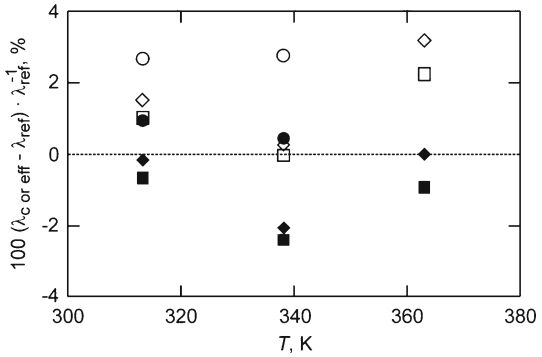

Fig. 3 Relative deviation of effective thermal conductivity λ_{eff} (*open symbols*) and thermal conductivity $\lambda_{\mathrm{c}} (= \lambda_{\mathrm{eff}} - \lambda_{\mathrm{r}})$ (*closed symbols*) from reference data λ_{ref} [35] for toluene as a function of temperature T for three different temperature differences (○ and ●, $\Delta T = 1$ K; ◇ and ◆, $\Delta T = 2$ K; □ and ■, $\Delta T = 3$ K) inside the fluid layer of 1 mm thickness of the guarded parallel-plate instrument

The parallel-plate instrument was checked by measuring the thermal conductivity of liquid toluene over a temperature range from (313.15 to 363.15) K in steps of 25 K. The results both with and without corrections for radiation are depicted in Fig. 3. They are in agreement with standard reference data for liquid toluene [35], where the maximum relative deviation of the corrected data does not exceed 2.5 %. With this result, the relative uncertainty ($k = 2$) of the thermal-conductivity data provided in this study can be estimated to be smaller than 3 %.

Before each filling of the thermal-conductivity cell with the dried IL samples, it was cleaned with ethanol, rinsed with deionized water, and dried by applying vacuum (0.5 mbar). For each sample, the thermal conductivity was measured at atmospheric pressure for a layer thickness of 1 mm and for temperatures ranging from (273.15 to 353.15) K in steps of 10 K. These temperatures represent mean values of the temperatures adjusted for the upper and lower plate surfaces contacting the liquid sample. For each mean temperature, the measurements were performed with temperature differences of (2 and 3) K between the two plate surfaces.

3 Results and Discussion

In the following, our results for the thermal conductivity of nine imidazolium-based ILs and one ammonium-based IL are summarized. In the first section, the experimental data are represented by empirical correlations and are discussed in comparison with literature. Then our results are analyzed in connection with a simple prediction method which could represent a convenient simplification in the acquisition of the thermal conductivity for the enormous amount of imaginable IL cation/anion combinations.

3.1 Experimental Data

The data obtained for the thermal conductivity λ_{c} of ILs in the temperature range from (273.15 to 353.15) K at atmospheric pressure are summarized in Table 4 and shown

Table 4 Thermal conductivity λ_c of the studied ILs at temperature T and atmospheric pressure

T (K)	λ_c ($W \cdot m^{-1} \cdot K^{-1}$)								
	273.15	283.15	293.15	303.15	313.15	323.15	333.15	343.15	353.15
[EMIM][OAc]	0.2137	0.2124	0.2110	0.2102	0.2066	0.2026	0.2002	0.1973	0.1915
[EMIM][$N(CN)_2$]	0.2053	0.2050	0.2021	0.2022	0.1986	0.1958	0.1942	0.1935	0.1914
[EMIM][$C(CN)_3$]	0.1956	0.1957	0.1930	0.1918	0.1900	0.1873	0.1868	0.1847	0.1815
[EMIM][$MeOHPO_2$]	0.1941	0.1948	0.1914	0.1959	0.1915	0.1906	0.1908	0.1917	0.1902
[EMIM][$Et(SO_4)$]	0.1876	0.1882	0.1856	0.1872	0.1840	0.1833	0.1832	0.1834	0.1830
[EMIM][$OcSO_4$]	0.1712	0.1711	0.1670	0.1679	0.1648	0.1629	0.1631	0.1626	0.1621
[EMIM][NTf_2]	0.1208	0.1206	0.1202	0.1215	0.1195	0.1184	0.1190	0.1194	0.1191
[HMIM][NTf_2]	0.1238	0.1224	0.1219	0.1237	0.1220	0.1201	0.1208	0.1212	0.1209
[BBIM][NTf_2]	0.1209	0.1203	0.1188	0.1198	0.1176	0.1170	0.1176	0.1171	0.1164
[OMA][NTf_2]	0.1314	0.1291	0.1299	0.1283	0.1266	0.1247	0.1244	0.1242	0.1248

in Fig. 4. Here, each data point represents the average value of two independent measurements for different temperature gradients inside the fluid layer between the two parallel plates of the instrument at the same mean temperature, cf. Sect. 2 and [36]. For all ILs and temperatures, the two single values showed a mean relative deviation of 0.52 %. The single relative deviations were clearly within the estimated relative expanded uncertainty of 3 % ($k = 2$) and did not exceed 2.04 %.

Figure 4 shows that for all ILs studied, the thermal conductivity slightly decreases with increasing temperature. The values of the thermal conductivity of the ILs can be found between (0.11 and 0.22) $W \cdot m^{-1} \cdot K^{-1}$ and are similar to those of common organic liquids at atmospheric pressure, see, e.g., chloroform (0.11079 $W \cdot m^{-1} \cdot K^{-1}$ at 303.15 K [37]), *n*-heptane (0.1254 $W \cdot m^{-1} \cdot K^{-1}$ at 293.25 K [38]), toluene (0.13088 $W \cdot m^{-1} \cdot K^{-1}$ at 298.15 K) [35], benzene (0.14156 $W \cdot m^{-1} \cdot K^{-1}$ at 295.921 K [39]), ethanol (0.1607 $W \cdot m^{-1} \cdot K^{-1}$ at 305.74 K [40]), and methanol (0.2038 $W \cdot m^{-1} \cdot K^{-1}$ at 292.3 K [30]). These findings correspond to the results available in the literature [12,19–25].

The drawn lines in Fig. 4 represent the correlation of our thermal-conductivity data as a function of temperature in the form of a linear equation,

$$\lambda_{c,calc} = \lambda_0 + \lambda_1 T, \tag{7}$$

where T is the temperature in K and λ_0 and λ_1 are the fit parameters given in Table 5. For the data correlation, the statistical weight of each data point has been assumed to be the same. As shown in the lower part of Fig. 4, the residuals of the thermal-conductivity data from the fit, Eq. 7, are clearly smaller than the expanded uncertainty ($k = 2$) of less than ±3 %. In Table 5, also the standard percentage deviation (root mean square, rms) of the measured thermal conductivities relative to those calculated by Eq. 7 is listed. For the measurements, the standard percentage deviation was in the range between (0.36 and 0.76) %.

For [EMIM][$EtSO_4$], [EMIM][NTf_2], and [HMIM][NTf_2], Fig. 5 shows a data comparison between our thermal-conductivity data and available literature data in the form of a deviation plot. Here, the correlation of our data, Eq. 7, serves as a basis.

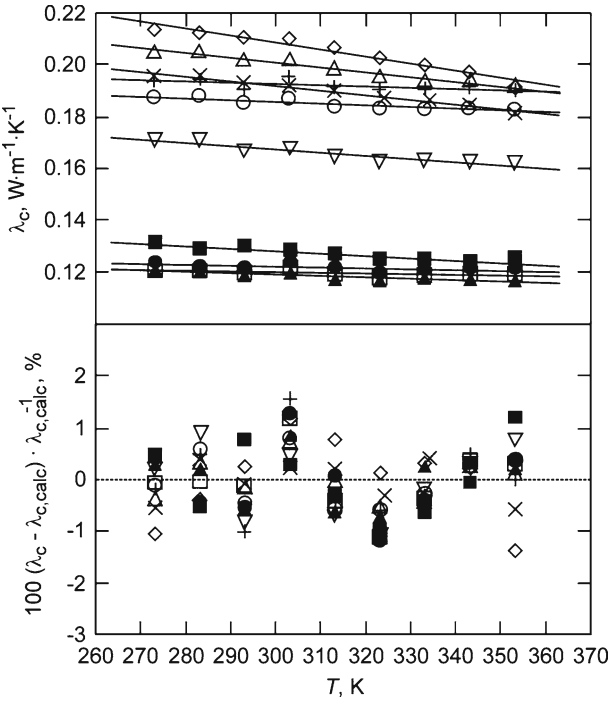

Fig. 4 Thermal conductivity λ_c of the studied ILs as a function of temperature T at atmospheric pressure and relative deviation of measured thermal conductivities λ_c from calculated data $\lambda_{c,calc}$ according to Eq. 7: ◇, [EMIM][OAc]; △, [EMIM][N(CN)$_2$]; ×, [EMIM][C(CN)$_3$]; +, [EMIM][MeOHPO$_2$]; ○, [EMIM][EtSO$_4$]; ▽, [EMIM][OcSO$_4$]; □, [EMIM][NTf$_2$]; ●, [HMIM][NTf$_2$]; ▲, [BBIM][NTf$_2$]; ■, [OMA][NTf$_2$]

Table 5 Coefficients of Eq. 7 for the thermal conductivity $\lambda_{c,calc}$ of the studied ILs

	λ_0 (W · m^{-1} · K^{-1})	λ_1 (W · m^{-1} · K^{-2})	rms[a]
[EMIM][OAc]	0.2903	-2.722×10^{-4}	0.76
[EMIM][N(CN)$_2$]	0.2573	-1.872×10^{-4}	0.40
[EMIM][C(CN)$_3$]	0.2451	-1.772×10^{-4}	0.36
[EMIM][MeOHPO$_2$]	0.2087	-5.233×10^{-5}	0.72
[EMIM][Et(SO$_4$)]	0.2067	-6.917×10^{-5}	0.48
[EMIM][OcSO$_4$]	0.2048	-1.245×10^{-4}	0.66
[EMIM][NTf$_2$]	0.1281	-2.650×10^{-5}	0.54
[HMIM][NTf$_2$]	0.1328	-3.500×10^{-5}	0.65
[BBIM][NTf$_2$]	0.1355	-5.467×10^{-5}	0.49
[OMA][NTf$_2$]	0.1561	-9.283×10^{-5}	0.70

[a] Standard percentage deviation of λ_c to the fit

For the further seven ILs studied in this work, no investigations are reported so far. The data comparison in Fig. 5 includes experimental data by Ge et al. [22], who measured the thermal conductivity of 11 ILs between (293 and 353) K at atmospheric pressure using an apparatus based on the transient hot-wire method with an estimated

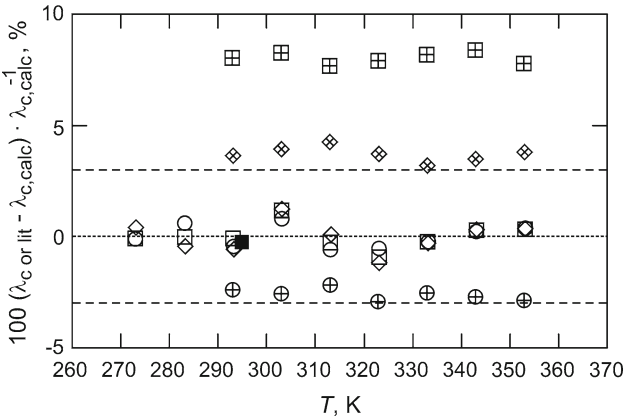

Fig. 5 Relative deviation of measured thermal conductivities λ_c and literature data λ_{lit} from calculated data $\lambda_{c,calc}$ according to Eq. 7: [EMIM][$EtSO_4$]: ○, this study; ⊕, Ge et al. [22]; [EMIM][NTf_2]: □, this study; ⊞, Ge et al. [22]; ■, Frez et al. [19]; [HMIM][NTf_2]: ◇, this study; ◈, Ge et al. [22]

uncertainty of less than $\pm 0.005\ W \cdot m^{-1} \cdot K^{-1}$. In the work of Ge et al. [22], the uncertainty of the temperature is estimated to be ±1 K. For [EMIM][NTf_2], an additional data point of Frez et al. [19] is depicted in Fig. 5. They performed thermal-diffusivity measurements for seven different ILs at a temperature of 296.85 K and atmospheric pressure with the transient grating technique. Typically, the standard percentage deviation of their experiments in determining the thermal diffusivity a was better than ±4 %. Frez et al. [19] found the thermal conductivity λ_c with a knowledge of density ρ and specific heat capacity c_p through $\lambda_c = a\rho c_p$. Based on their measured thermal diffusivity $a(= 0.601 \times 10^{-7}\ m^2 \cdot s^{-1})$, they have calculated the thermal conductivity of [EMIM][NTf_2] to be $(0.120 \pm 0.005)\ W \cdot m^1 \cdot K^{-1}$. As can be seen from Fig. 5, the datum given by Frez et al. [19] for [EMIM][NTf_2] at 296.85 K shows excellent agreement with our data set. For [EMIM][$EtSO_4$] and [HMIM][NTf_2], within combined uncertainties also agreement can be found between our data and those of Ge et al. [22]. In contrast to this, their data for [EMIM][NTf_2] deviate with respect to Eq. 7 as well as to the datum of Frez et al. [19] by more than +8 %, which is outside the estimated combined uncertainties. Figure 5 shows an increasing deviation of the data sets of Ge et al. [22] from the data of this study with decreasing dynamic viscosity η (= 125.4 mPa · s for [EMIM][$EtSO_4$] at 293.15 K [34], = 38.6 mPa · s for [EMIM][NTf_2] at 293.15 K [34], and = 89.26 mPa · s for [HMIM][NTf_2] at 293.15 K [41]). The reason for this may be an underestimated contribution of convective heat transfer for the transient hot-wire apparatus used by Ge et al. [22]. For the systematically slightly higher values reported by Ge et al. [22] for the thermal conductivity of [HMIM][NTf_2] and [EMIM][NTf_2] in comparison to those obtained in this work, different sample purities may be a possible reason. Ge et al. [22] showed that small levels of water or halide, which are common impurities from the synthesis of ILs, both increase the thermal conductivity. Yet, in their study the water content was found to be less than 80 ppm and the chloride mass fraction was less than 5×10^{-6}, which indicates lower purity samples utilized in our study.

3.2 Prediction of the Thermal Conductivity of ILs

For predicting the thermal conductivity of ILs, our interest was directed to an analysis of the present results in connection with the molecular structure. While for the $[NTf_2]$-based ILs a slight increase of the thermal conductivity with increasing molar mass is found at a given temperature, the [EMIM]-based ILs show a pronounced, approximately linear decrease. This behavior is shown in Fig. 6a for a temperature of 293.15 K. For the $[NTf_2]$-based ILs, the small increase of the thermal conductivity with increasing chain length of the cation is probably due to internal vibration modes, which are important for heat conduction in addition to translation modes. In the case of the [EMIM]-based ILs, the effect of these vibration modes could be decreasing with increasing molecular size of the anion. This interpretation would be in agreement with the observed decreasing thermal conductivity with increasing molar mass.

For finding a simple prediction method for the thermal conductivity λ_c of ILs, we plotted different combinations of our data with other thermophysical properties, e.g., dynamic viscosity η and density ρ, as a function of the molar mass M as depicted in Fig. 6b to d. This approach was motivated by the study of Tomida et al. [21], who proposed a relationship between $\lambda_c M/\eta$ and M in the form of $\log(\lambda_c M/\eta) = A - BM$, where A and B are fitting parameters obtained by least-squares fitting. The correlation by Tomida et al. [21], however, is based on their own experimental thermal-conductivity data of the transient hot-wire technique for three $[PF_6]$ (hexafluorophosphate)-based ILs [21] having the cations [BMIM], [HMIM], or [OMIM] (1-methyl-3-octylimidazolium) and for [BMIM][BF_4] (1-butyl-3-methylimidazolium tetrafluoroborate) [20] as well as on literature data for numerous n-alkanes ranging from n-pentane to n-tetradecane. For correlating the n-alkanes and ILs together, Tomida et al. [21] assumed that the molar mass of the ILs is two times larger than the true value.

Figure 6b shows a logarithmic plot of $\lambda_c\ M/\eta$ as a function of M at 293.15 K and atmospheric pressure for the ten ILs studied in this work. For this, data for the dynamic viscosity were used from our previous work [28,34], with the exception of [HMIM][NTf_2], [EMIM][OAc], and [EMIM][$C(CN)_3$]. For these ILs, corresponding data of 89.26 mPa · s at 293.15 K, 93 mPa · s at room temperature, and 18 mPa · s at 295.15 K were adopted from [41], http://www.basionics.com/en/ionic-liquids/products/data/bc01.htm, and [42], respectively. It can be seen that a relationship between $\lambda_c\ M/\eta$ and M as proposed by Tomida et al. [21] is different for the cation variation in $[NTf_2]$ and for the anion variation in [EMIM]-based ILs. Furthermore, for the latter, there is no clear trend of decreasing values for $\lambda_c\ M/\eta$ with increasing molar mass. For the anion variation in [EMIM]-based ILs—with the exception of [EMIM][NTf_2]—combining only thermal-conductivity data λ_c and molar mass M, a distinct trend in the form of a linear relationship between $\lambda_c\ M$ and M could be observed, see Fig. 6c. Yet, again the trends are different for the anion variation in [EMIM] and the cation variation in $[NTf_2]$-based ILs. In contrast to this, combining thermal conductivity λ_c with density ρ and molar mass M by plotting $\lambda_c\ M\ \rho$ as a function of the molar mass M, see Fig. 6d, a single common trend is observable for all systems under investigation. This result suggests that the thermal conductivity of an arbitrary IL can simply be predicted from

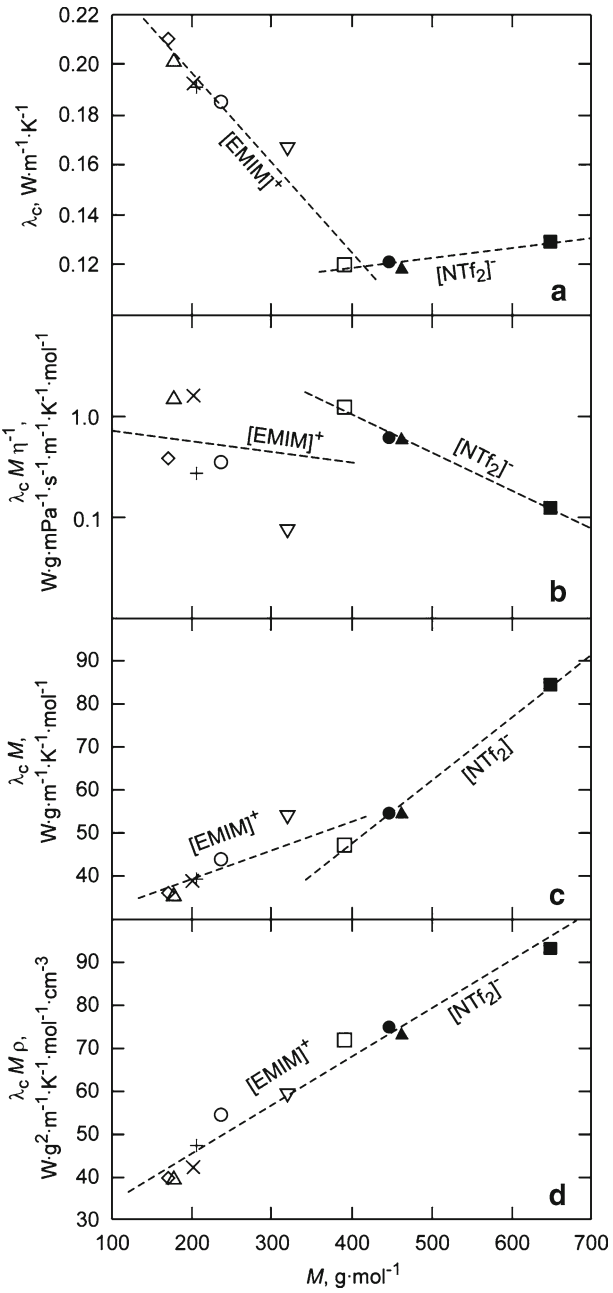

Fig. 6 Thermal conductivity λ_c and its combination with further thermophysical properties for the studied ILs at $T = 293.15$ K and atmospheric pressure as a function of the molar mass M: (a) thermal conductivity λ_c; (b) product of thermal conductivity λ_c and molar mass M divided by dynamic viscosity η; (c) product of thermal conductivity λ_c and molar mass M; and (d) product of thermal conductivity λ_c, molar mass M, and density ρ; ◇, [EMIM][OAc]; △, [EMIM][$N(CN)_2$]; ×, [EMIM][$C(CN)_3$]; +, [EMIM][$MeOHPO_2$]; ○, [EMIM][$EtSO_4$]; ▽, [EMIM][$OcSO_4$]; □, [EMIM][NTf_2]; ●, [HMIM][NTf_2]; ▲, [BBIM][NTf_2]; ■, [OMA][NTf_2]

$$\lambda_{c,\text{prediction}} M\rho = AM + B, \tag{8}$$

where the parameters $A = 0.1130\ \text{g} \cdot \text{cm}^{-3} \cdot \text{W} \cdot \text{m}^{-1} \cdot \text{K}^{-1}$ and $B = 22.65\ \text{g}^2 \cdot \text{cm}^{-3} \cdot \text{W} \cdot \text{m}^{-1} \cdot \text{K}^{-1} \cdot \text{mol}^{-1}$ were obtained by least-squares fitting of our results at a temperature of 293.15 K and atmospheric pressure. For a quantitative prediction of the thermal conductivity in units of $\text{W} \cdot \text{m}^{-1} \cdot \text{K}^{-1}$ by Eq. 8, the molar mass M and density ρ have to be used in units of $\text{g} \cdot \text{mol}^{-1}$ and $\text{g} \cdot \text{cm}^{-3}$. For all ILs studied in this work, the standard percentage deviation and mean absolute percentage deviation of the experimental thermal-conductivity data at a temperature of 293.15 K and atmospheric pressure from those calculated with Eq. 8 are 5.5 and 4.6. For [EMIM][$EtSO_4$], a maximum relative deviation of 10.2 % is found. Due to the low temperature dependence of the thermal conductivity in the studied temperature range, no reasonable correlation for this dependence in connection with the molecular structure could be found. The simple prediction method suggested here, however, seems to be able to provide valuable tendencies for the thermal conductivity of arbitrary ILs in the temperature range considered here.

For setting up Eq. 8, density data provided in our former studies [28,36] could be used, except for [EMIM][OAc], [EMIM][$C(CN)_3$], and [HMIM][NTf_2]. For the latter, densities were measured within this study using the vibrating-tube method with an estimated expanded relative uncertainty ($k = 2$) of less than ±0.02 %. More details on the method and the used instrument (DMA 5000, Anton Paar) can be found in [28,36]. The measurements were performed at atmospheric pressure starting from (273.15 to 363.15) K in steps of 5 K. The density data are given in Table 6 and were correlated with second-order polynomial functions,

$$\rho_{\text{calc}} = \rho_0 + \rho_1 T + \rho_2 T^2. \tag{9}$$

Table 7 shows the correlation coefficients ρ_0, ρ_1, and ρ_2 as well as the standard percentage deviation (rms) of the experimental density data to the fit. The resulting rms values were distinctly smaller than the relative uncertainty for the density measurements.

To the best of our knowledge, no density data for [EMIM][OAc] and [EMIM][$C(CN)_3$] are available in the literature to date. [HMIM][NTf_2] is an IUPAC reference substance, for which densities were measured in a round-robin study using high-purity samples from the same batch with a nominal purity of >99.5 % on a molar basis [43,44]. The recommended values were expressed by a linear equation for the temperature range from (258 to 373) K. For all temperatures, the combined expanded uncertainty ($k = 2$) of this equation was estimated to be 0.1 % [44]. In addition, it was shown that the deviations of nearly all further data sets available in the literature are negative. This was mainly attributed to impurities in the corresponding samples. The presented deviations from the IUPAC equation range from about (+0.05 % to −0.6) %, and one datum even deviates by more than −1.2 % [44]. The deviations of other recent density data for [HMIM][NTf_2] provided by Jacquemin et al. [45], Tariq et al. [46], and Ahosseini et al. [47] are in the range between (−0.03 and −0.24) %. Our data presented in Table 6 deviates by (−0.50 to −0.58) % from the equation recommended in the IUPAC study, which is distinctly outside the combined uncertainties. As the calibration of our densimeter was successfully checked with deionized water

Table 6 Density ρ of [EMIM][OAc], [EMIM][C(CN)$_3$], and [HMIM][NTf$_2$] at temperature T and atmospheric pressure

T (K)	ρ (g · cm^{-3})		
	[EMIM][OAc]	[EMIM][C(CN)$_3$]	[HMIM][NTf$_2$]
273.15	1.11531	1.09928	1.38784
278.15	1.11213	1.09568	1.38306
283.15	1.10896	1.09207	1.37845
288.15	1.10580	1.08849	1.37385
293.15	1.10269	1.08491	1.36927
298.15	1.09968	1.08137	1.36469
303.15	1.09664	1.07784	1.36012
308.15	1.09360	1.07432	1.35556
313.15	1.09057	1.07082	1.35101
318.15	–	1.06734	–
323.15	1.08452	1.06388	1.34194
328.15	1.08152	1.06043	1.33743
333.15	1.07852	1.05700	1.33293
338.15	1.07554	1.05358	1.32845
343.15	1.07257	1.05018	1.32397
348.15	1.06960	1.04680	1.31952
353.15	1.06665	1.04342	1.31507
358.15	1.06371	1.04007	1.31064
363.15	1.06078	1.03673	1.30622

Table 7 Coefficients of Eq. 9 for the density ρ of [EMIM][OAc], [EMIM][C(CN)$_3$], and [HMIM][NTf$_2$]

	ρ_0 (g · cm^{-3})	ρ_1 (g · cm^{-3} · K^{-1})	ρ_2 (g · cm^{-3} · K^{-2})	rms[a]
[EMIM][OAc]	1.30502	-7.6268×10^{-4}	2.4838×10^{-7}	0.0037
[EMIM][C(CN)$_3$]	1.32173	-9.0419×10^{-4}	3.2882×10^{-7}	0.0004
[HMIM][NTf$_2$]	1.66112	-1.0721×10^{-3}	2.6106×10^{-7}	0.0019

[a] Standard percentage deviation of ρ to the fit

and air before and after the measurements for each IL, these large deviations must be attributed to the impurities in the [HMIM][NTf$_2$] sample.

Taking into account in addition to our data all experimental data available until now in the literature for the thermal conductivity of ILs at a temperature of 293.15 K and atmospheric pressure [12,20–25], the fitting parameters in Eq. 8 could be determined to be $A = 0.1244\,\mathrm{g \cdot cm^{-3} \cdot W \cdot m^{-1} \cdot K^{-1}}$ and $B = 18.84\,\mathrm{g^2 \cdot cm^{-3} \cdot W \cdot m^{-1} \cdot K^{-1} \cdot mol^{-1}}$. In this case, the standard percentage deviation of the thermal-conductivity data from those calculated with Eq. 8 is 7.8 %.

For setting up the correlation Eq. 8 including literature data, density data were used from the respective literature if given therein [12,20,24,25]. It should be noted

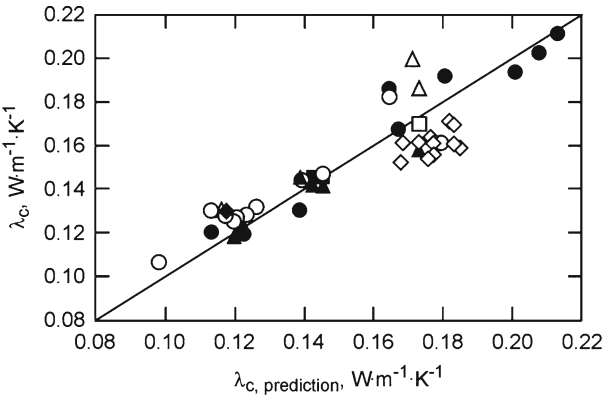

Fig. 7 Linear relationship between experimental thermal conductivity λ_c and predicted thermal conductivity $\lambda_{c,\ prediction}$ using Eq. 8 with $A = 0.1244\ g \cdot cm^{-3} \cdot W \cdot m^{-1} \cdot K^{-1}$ and $B = 18.84\ g^2 \cdot cm^{-3} \cdot W \cdot m^{-1} \cdot K^{-1} \cdot mol^{-1}$: ●, this study; △, Van Valkenburg et al. [12]; □, Tomida et al. [20]; ■, Tomida et al. [21]; ○, Ge et al. [22]; ♦, Chen et al. [23]; ▲, Nieto de Castro et al. [24]; ◇, Gardas et al. [25]

that the thermal conductivity and density data for [BMIM][PF_6], [HMIM][PF_6], and [OMIM][PF_6] from Tomida et al. [21], who have studied the ILs at three temperatures in the range between (294 and 335) K, were extrapolated to 293.15 K. For processing the results of another study of Tomida et al. [20], the density for [BMIM][BF_4] was adopted from the study of Van Valkenburg et al. [12]. For the study of Ge et al. [22], the densities for [NTf_2]-based ILs having the cations [EMIM], [BMIM], [HMIM], [OMIM], [DMIM] (1-decyl-3-methylimidazolium), [C4mpyrr] (1-butyl-1-methylpyrrolidinium), or [$(C_6H_{13})_3P(C_{14}H_{29})$] (trihexyl(tetradecyl)phosphonium) as well as for [$(C_6H_{13})_3P(C_{14}H_{29})$]Cl (trihexyl(tetradecyl)phosphonium chloride), [EMIM][$EtSO_4$], [BMIM][OTf] (1-butyl-3-methylimidazolium trifluoromethanesulfonate), and [C4mpyrr][FAP] (1-butyl-1-methylpyrrolidinium tris(pentafluoroethyl)trifluorophosphate) were adopted from [34,45,48–54], respectively. For the datum given by Chen et al. [23] for [BMIM][NTf_2], the density was also adopted from [48].

Figure 7 shows good agreement of the predicted thermal conductivity $\lambda_{c,\ prediction}$ with the corresponding experimental thermal conductivity λ_c of the ILs studied until now in literature [12,20–25] and in this study at a temperature of 293.15 K and atmospheric pressure. For the 45 data points of 36 ILs, the standard percentage deviation and mean absolute percentage deviation of the experimental data from the prediction is 7.8 and 6.5. The maximum relative deviation between the predicted and experimental thermal-conductivity data is 16.6 %, which can be observed for the data point given by Van Valkenburg et al. [12] for [EMIM][BF_4].

4 Conclusions

For nine imidazolium-based ILs and one tetraalkylammonium-based IL, the thermal conductivity has been determined with a steady state parallel-plate instrument in the

temperature range between (273.15 and 353.15) K at atmospheric pressure with an uncertainty of ±3 %. The thermal conductivity of the ILs is only weakly dependent on temperature. The decrease of the thermal conductivity with increasing temperature can well be represented by a linear correlation. For the anion variation in [EMIM]-based ILs, the thermal conductivity decreases with the size of the anion. For the cation variation in $[NTf_2]$-based ILs, the thermal conductivity increases somewhat with the size of the cation. Thus, for the dependence of the thermal conductivity of ILs on their molar mass, two different trends are observable. For all ILs, the thermal conductivity could be predicted from a linear relation between thermal conductivity, molar mass, and density. The simple prediction represents all experimental thermal-conductivity data available in the literature until now with a standard deviation of less than 8 %. Thus, it seems to conveniently provide reliable estimates for the thermal conductivity of arbitrary ILs.

Acknowledgments This work was supported by the German Research Foundation (Deutsche Forschungsgemeinschaft, DFG) by funding the Erlangen Graduate School in Advanced Optical Technologies (SAOT) within the German Excellence Initiative and via the DFG-SPP1191 priority program, grants FR 1709/9-1 and WA 1615/8-2, and by the Max-Buchner-Forschungsstiftung. We thank Solvent Innovation GmbH, Germany, BASF AG, Germany, and Lonza Cologne AG, Germany, for providing some of the investigated ILs.

References

1. T. Torimoto, T. Tsuda, K. Okazaki, S. Kuwabata, Adv. Mater. **22**, 1196 (2010)
2. M. Armand, F. Endres, D.R. MacFarlane, H. Ohno, B. Scrosati, Nat. Mater. **8**, 621 (2009)
3. J.F. Wishart, Energy Environ. Sci. **2**, 956 (2009)
4. N.V. Plechkova, K.R. Seddon, Chem. Soc. Rev. **37**, 123 (2008)
5. O.A. El Seoud, A. Koschella, L.C. Fidale, S. Dorn, T. Heinze, Biomacromolecules **8**, 2629 (2007)
6. H. Zhao, Chem. Eng. Commun. **193**, 1660 (2006)
7. C. Chiappe, D. Pieraccini, J. Phys. Org. Chem. **18**, 275 (2005)
8. P. Wasserscheid, W. Keim, Angew. Chem. Int. Ed. **39**, 3772 (2000)
9. C. Jork, C. Kristen, D. Pieraccini, A. Stark, C. Chiappe, Y.A. Beste, W. Arlt, J. Chem. Thermodyn. **37**, 537 (2005)
10. H. Sakaebe, H. Matsumoto, K. Tatsumi, Electrochim. Acta **53**, 1048 (2007)
11. A.-E. Jiménez, M.-D. Bermúdez, Tribol. Lett. **26**, 53 (2007)
12. M.E. Van Valkenburg, R.L. Vaughn, M. Williams, J.S. Wilkes, Thermochim. Acta **425**, 181 (2005)
13. J.S. Wilkes, in *Ionic Liquids in Synthesis*, ed. by P. Wasserscheid, T. Welton (Wiley-VCH, Weinheim, 2003), p. 2
14. K. Tochigi, H. Yamamoto, J. Phys. Chem. C **111**, 15989 (2007)
15. S. Zhang, N. Sun, X. He, X. Lu, X. Zhang, J. Phys. Chem. Ref. Data **35**, 1475 (2006)
16. M. Deetlefs, K.R. Seddon, M. Shara, Phys. Chem. Chem. Phys. **8**, 642 (2006)
17. R.L. Gardas, J.A.P. Coutinho, AIChE J. **55**, 1274 (2009)
18. J.M.P. França, C.A. Nieto de Castro, M.M. Lopes, V.M.B. Nunes, J. Chem. Eng. Data **54**, 2569 (2009)
19. C. Frez, G.J. Diebold, C.D. Tran, S. Yu, J. Chem. Eng. Data **51**, 1250 (2006)
20. D. Tomida, S. Kenmochi, T. Tsukada, C. Yokoyama, Netsu Bussei **20**, 173 (2006)
21. D. Tomida, S. Kenmochi, T. Tsukada, K. Qiao, C. Yokoyama, Int. J. Thermophys. **28**, 1147 (2007)
22. R. Ge, C. Hardacre, P. Nancarrow, D.W. Rooney, J. Chem. Eng. Data **52**, 1819 (2007)
23. H. Chen, Y. He, J. Zhu, H. Alias, Y. Ding, P. Nancarrow, C. Hardacre, D. Rooney, C. Tan, Int. J. Heat Fluid Flow **29**, 149 (2008)
24. C.A. Nieto de Castro, M.J.V. Lourenço, A.P.C. Ribeiro, S.I.C. Vieira, P. Goodrich, C. Hardacre, J. Chem. Eng. Data **55**, 653 (2010)

25. R.L. Gardas, R. Ge, P. Goodrich, C. Hardacre, A. Hussain, D.W. Rooney, J. Chem. Eng. Data **55**, 1505 (2010)
26. F. Maier, J.M. Gottfried, J. Rossa, D. Gerhard, P.S. Schulz, W. Schwieger, P. Wasserscheid, H.-P. Steinrück, Angew. Chem. Int. Ed. **45**, 7778 (2006)
27. S. Himmler, S. Hörmann, R. van Hal, P.S. Schulz, P. Wasserscheid, Green Chem. **8**, 887 (2006)
28. B. Hasse, J. Lehmann, D. Assenbaum, P. Wasserscheid, A. Leipertz, A.P. Fröba, J. Chem. Eng. Data **54**, 2576 (2009)
29. J.H. Davis, C.M. Gordon Jr., C. Hilgers, P. Wasserscheid, in *Ionic Liquids in Synthesis*, ed. by P. Wasserscheid, T. Welton (Wiley-VCH, Weinheim, 2006), p. 7
30. Ya.M. Naziev, M.M. Bashirov, I.M. Abdulagatov, Fluid Phase Equilib. **226**, 221 (2004)
31. R. Braun, S. Fischer, A. Schaber, Wärme Stoffübertrag. **17**, 121 (1983)
32. M. Kohler, Z. Angew. Phys. **18**, 356 (1965)
33. H. Poltz, Int. J. Heat Mass Transf. **8**, 515 (1965)
34. A.P. Fröba, H. Kremer, A. Leipertz, J. Phys. Chem. B **112**, 12420 (2008)
35. M.L.V. Ramires, C.A. Nieto de Castro, R.A. Perkins, Y. Nagasaka, A. Nagashima, M.J. Assael, W.A. Wakeham, J. Phys. Chem. Ref. Data **29**, 133 (2000)
36. A.P. Fröba, M.H. Rausch, K. Krzeminski, A. Leipertz, Int. J. Heat Mass Transfer (to be submitted) (2011)
37. R.L. Rowley, S.-C. Yi, D.V. Gubier, J.M. Stoker, J. Chem. Eng. Data **33**, 362 (1988)
38. C.A. Nieto de Castro, J.C.G. Calado, W.A. Wakeham, M. Dix, J. Phys. E **9**, 1073 (1976)
39. H. Watanabe, H. Kato, J. Chem. Eng. Data **49**, 809 (2004)
40. M.J. Assael, E. Charitidou, C.A. Nieto de Castro, Int. J. Thermophys. **9**, 813 (1988)
41. J.A. Widegren, J.W. Magee, J. Chem. Eng. Data **52**, 2331 (2007)
42. Y. Yoshida, K. Muroi, A. Otsuka, G. Saito, M. Takahashi, T. Yoko, Inorg. Chem. **43**, 1458 (2004)
43. K.N. Marsh, J.F. Brennecke, R.D. Chirico, M. Frenkel, A. Heintz, J.W. Magee, C.J. Peters, L.P.N. Rebelo, K.R. Seddon, Pure Appl. Chem. **81**, 781 (2009)
44. R.D. Chirico, V. Diky, J.W. Magee, M. Frenkel, K.N. Marsh, Pure Appl. Chem. **81**, 791 (2009)
45. J. Jacquemin, R. Ge, P. Nancarrow, D.W. Rooney, M.F. Costa Gomes, A.A.H. Pádua, C. Hardacre, J. Chem. Eng. Data **53**, 716 (2008)
46. M. Tariq, P.A.S. Forte, M.F. Costa Gomes, J.N. Canongia Lopes, L.P.N. Rebelo, J. Chem. Thermodyn. **41**, 790 (2009)
47. A. Ahosseini, B. Sensenich, L.R. Weatherley, A.M. Scurto, J. Chem. Eng. Data **55**, 1611 (2010)
48. K.R. Harris, M. Kanakubo, L.A. Woolf, J. Chem. Eng. Data **52**, 1080 (2007)
49. J.M.S.S. Esperança, H.J.R. Guedes, J.N.Ganongia Lopes, L.P.N. Rebelo, J. Chem. Eng. Data **53**, 867 (2008)
50. R.L. Gardas, M.G. Freire, P.J. Carvalho, I.M. Marrucho, I.M.A. Fonseca, A.G.M. Ferreira, J.A.P. Coutinho, J. Chem. Eng. Data **52**, 1881 (2007)
51. L.I.N. Tome, P.J. Carvalho, M.G. Freire, I.M. Marrucho, I.M.A. Fonseca, A.G.M. Ferreira, J.A.P. Coutinho, R.L. Gardas, J. Chem. Eng. Data **53**, 1914 (2008)
52. R.L. Gardas, H.F. Costa, M.G. Freire, P.J. Carvalho, I.M. Marrucho, I.M.A. Fonseca, A.G.M. Ferreira, J.A.P. Coutinho, J. Chem. Eng. Data **53**, 805 (2008)
53. J.M.S.S. Esperança, H.J.R. Guedes, M. Blesic, L.P.N. Rebelo, J. Chem. Eng. Data **51**, 237 (2006)
54. R.L. Gardas, M.G. Freire, P.J. Carvalho, I.M. Marrucho, I.M.A. Fonseca, A.G.M. Ferreira, J.A.P. Coutinho, J. Chem. Eng. Data **52**, 80 (2007)